SUBUNIT INTERACTIONS AND THE ALLOSTERIC RESPONSE IN PHOSPHORYLASE

S. Sprang and R. J. Fletterick, *Department of Biochemistry and Biophysics, University of California at San Francisco, San Francisco, California 94143 U.S.A.*

ABSTRACT: The contribution of intersubunit interactions to allosterically induced conformational changes in phosphorylase are considered. Phorphorylase *a*, P*a* (phosphorylated at Ser-14), is significantly in the active (R) conformation, while phosphorylase *b*, P*b* (nonphosphorylated), is predominantly in the inactive (T) conformation. The structure of glucose-inhibited (T) P*a* has been determined at 2.5-Å resolution and atomic coordinates have been measured. These data have been used to calculate the solvent accessible surface area at the subunit interface and map noncovalent interactions between protomers. The subunit contact involves only 6% of the P*a* monomer surface, but withdraws an area of 4,600 Å^2 from solvent. The contact region is confined to the N-terminal (regulatory) domain of the subunit. Half of the residues involved are among the 70 N-terminal peptides. A total of ~ 100 atoms take part in polar or nonpolar contacts of < 4.0 Å with atoms of the symmetry-related monomer. The contact surface surrounds a central cavity at the core of the interface of sufficient volume to accommodate 150-180 solvent molecules. There are four intersubunit salt bridges. Two of these (Arg 10/Asp 32, Ser-14-P/Arg 43) are interactions between the N-terminus of one protomer with an α-helix loop segment near the N-terminus of the symmetry-related molecule. These two are relatively solvent accessible. The remainder (Arg 49/Glu 195, Arg 184/Asp 251) are nearer the interface core and are less accessible. The salt bridges at the N-terminus are surrounded by the polar and nonpolar contacts which may contribute to their stability. Analysis of the difference electron density betwen the isomorphous P*a* and P*b* crystal structures reveals that the N-terminal 17 residues of P*b* are disordered. P*b* thus lacks two intermolecular and one intrasubunit (Ser-14-P/Arg 69) salt linkage present in P*a*. The absence of these interactions in P*b* is manifested in the difference in the free energy of T → R activation, which is 4 kcal more than that for P*a*. Difference Fourier analysis of the T → R transition in substrate-activated crystals of P*a* suggests that the 70 N-terminal residues undergo a concerted shift towards the molecular core; salt bridges are probably conserved in the transition. It is proposed that the N-terminus, when "activated" by phosphorylation (via a specific kinase) behaves as an intramolecular "effector" of the R state in phosphorylase and serves as the vehicle of homotropic cooperativity between subunits of the dimer.

INTRODUCTION

In the simplest models, subunits of allosteric oligomers are presumed to exist in either of two conformations, T or R, of which the latter exclusively exhibits binding affinity for substrates and, possibly, catalytic activity. The interaction of positive effector ligands with one subunit is associated with a substantial shift in the T / R equilibrium to the right. Positive cooperativity arises when a T → R transition in one subunit decreases the free energy of to the R state with respect to the T state in the remaining subunits, thereby increasing their respective substrate or ligand affinities. The Monod-Wyman-Changeux (MWC)(1) and Adair-Koshland-Nemethy-Filmer (AKNF)(2, 3) models of allostery were developed essentially from equilibrium binding and kinetic information. The classic MWC scheme requires symmetry among the subunits to be conserved throughout the binding sequence; the AKNF model does not, and

thereby allows for negative cooperativity. These models place only a few restrictions on the physical events which mediate cooperativity or changes in the structure of the monomers. Indeed, any model must assume protomers in noncovalent contact. However, dynamic processes such as "induced fit" (4) are not predicted by the binding data and are ultimately irrelevant to the equilibrium models.

From a structural viewpoint, allostery is effected through conformational changes which link ligand binding sites to subunit interfaces. The free energy changes expressed as alteration of ligand binding affinities are associated with changes in conformation of the interface between cooperative subunits. Structural information concerning the nature of these interactions was not available at the time the first models of allostery were proposed. Since that time, subunit interactions in only a few allosteric systems, notably the hemoglobin tetramer (5, 6) and tobacco mosaic virus (TMV) (7), have been considered in detail. These studies have suggested that salt linkages, i.e., noncovalent bonds linking charged groups, are particularly important in the "transmission" of allosterically induced conformational changes in cooperative oligomers. More accurately, subunit stabilization energies depend on salt bridges at the interacting interfaces (8). Chothia has emphasized the importance of the hydrophobic effect as an alternate or additional source of stability (9). In this report, we pose the problem of relating the subunit interactions and allosteric response in rabbit muscle phosphorylase *a*, a cooperative dimer.

Phosphorylase is an exquisitely regulated enzyme which catalyzes the breakdown of glycogen to glucose-1-phosphate. The enzyme is physiologically active as a dimer of 198,000 daltons and undergoes a T / R equilibrium regulated in vivo by about 10 different allosteric effectors. The most important "effector" is a covalent phosphorylation of Ser 14. The predominantly inactive (T) phosphorylase *b* (P*b*) is converted to active (significantly R) phosphorylase *a* (P*a*) by a specific kinase. This phosphoryl moiety can be considered one locus of allosteric regulation. As the primary glucose receptor in the liver (10), both the *a* and *b* enzymes are subject to an intricate array of hormonal, metabolic, and "energy feedback" controls. In addition to the site of covalent modification, there are three distinct positive effector binding sites (for glycogen, Pi, G-1-P, AMP) which promote the catalytically active R conformation, and three sites which bind negative effectors (glucose, purines, ATP) and stabilize the inactive T-conformation. The regulation of phosphorylase is discussed in greater detail elsewhere (11–13).

The three-dimensional structure of glucose-inhibited (T) P*a* has been determined at a resolution of 2.5 Å, and coordinates for the ~ 14,000 atoms of the dimer have been measured (14). The structure is currently being refined at higher resolution with an extended 2.1-Å data set. P*b*, also in the T conformation, has been determined at 3.0-Å resolution by Weber et al. (15). Since the two enzymes crystallize in identical unit cells, a direct comparison of the two structures is straightforward, and has been reported at 6.0-Å resolution (16). This analysis has demonstrated that the tertiary structures of the two enzymes are almost completely homologous at this resolution, except at the N-terminal tail, which lies along the dimer interface and contains the locus of covalent modification, Ser 14. The T → R transition in phosphorylase *a* has also been subjected to crystallographic analysis (17). When glucose is replaced by the substrate glucose-1-phosphate (G-1-P) in the presence of the substrate maltoheptaose or AMP (a positive effector of the R state), the enzyme undergoes a T → R transition within the crystal. Although this change introduces considerable disorder in the crystal lattice, the structural change can be followed at low resolution and is shown to consist of a major reordering of the polypeptide chain at the intersubunit domain and other changes near the glucose, purine, and glycogen binding sites.

In this discussion, we examine in detail the subunit interactions between protomers of T state P*a*. We then attempt to discern which interactions might be conserved by the T → R transition and to discover where changes in the subunit interactions occur and which residues are involved. This information is particularly important in characterizing the entropic and enthalpic changes arising from interactions at the subunit interface and therefore the contribution to the free energy difference between T and R states. Since phosphorylation of (the N-terminal) Ser 14 markedly changes the T / R equilibrium, we ask how such modification alters noncovalent interactions at the dimer interface.

METHODS

Rabbit muscle phosphorylase *a* has been crystallized in the presence of 50 mM glucose in the tetragonal space group $P4_32_12$ (18) with the two-fold axis of the physiological dimer coincident with the crystallographic axis at $x = y$ (16). The molecular structure of the enzyme has been determined at 2.5-Å resolution by a multiple isomorphous replacement (MIR) phasing procedure, and coordinates have been measured for nonhydrogen atoms of the 837 residues from Ser 5 to the C-terminus. The crystallographic R value for this model is 0.44 for the 2.5-Å data. Details concerning the structure solution are given elsewhere (14). All calculations presented here have been carried out with the coordinates described above. The model is currently being subjected to crystallographic refinement using the conjugate gradient procedure of Jack and Levitt (19) with the data set extended to 2.1-Å resolution. P*a* and P*b* have been compared at 6.0-Å resolution by difference Fourier analysis using MIR phases derived for P*a* (16).

Crystallographic analysis of the T → R confromational transition in P*a* has also been described (17). Crystals in which a significant fraction of P*a* assumes the R-state can be prepared by allowing glucose to diffuse from the lattice and subsequently soaking the crystals in a solution of the substrates 50 mM G-1-P and 200 mM maltoheptaose. This treatment normally causes the crystals to shatter; in favorable cases the crystals reanneal to a state of sufficient lattice order to allow measurement of low resolution diffraction data. The structural changes are analyzed by difference Fourier analysis with coefficients $(F_s\text{-}F_{Nat})$, where subscripts refer to the substrate perturbed and native structures, respectively. Evaluation of the gradient of the difference electron density at the Cα position for each P*a* residue allows a determination of the extent and connectivity of the structural changes (17).

Subunit interactions have been analyzed by identifying probable noncovalent contacts between the protomers and characterizing them as nonpolar, polar, or salt bridge (charge) interactions. Since the P*a* coordinate set is subject to average errors of 0.5–1.0 Å for surface atoms in the region of the subunit interface, contacts cannot be well defined. For this reason, we assume that atom pairs across the interface separated by < 4.0 Å are involved in some interaction. Contact distances of < 5.0 Å between charged atoms are accepted as evidence of probable interactions. Polar contacts include hydrogen bonds, salt bridges, but also any (N,N) or (O,O) contact, regardless of the presumed charge or protonation state of the atoms involved. Nonpolar interactions involve all contacts of C with (N,C,O) also without regard to the charges of the heteroatoms. Atoms of a reference P*a* monomer which are involved in the subunit contact are displayed on a projection (perpendicular to the crystallographic *c* axis) of the interface.

Subunit interactions are also defined by the difference in solvent accessible surface area in square Ångstroms, ΔA_s, between a given residue in an isolated monomer and in the dimer. These calculations are carried out according to the method of Lee and Richards (20) using the program of T. J. Richmond.[1] Residues for which $\Delta A_s \leq 30.0$ Å^2 are to some extent, "buried" at the dimer interface and so are assumed to be involved in the subunit interaction. We emphasize that ΔA_s is not intended to represent the change in accessible surface a residue undergoes in the monomer → dimer transition, since the monomers certainly undergo some structural changes on dimerization.

The solvent accessible volume within the dimer interface is mapped by the sum function introduced by Greer and Bush (21). The sum function is evaluated over the region of the dimer interface and gives

[1]Personal communication.

the value of the volume, V_{ij}, for all volume elements centered at every x_i,y_i on the interface contact surface.

The sum function (Fig. 3) has been calculated by adding a probe radius of 1.35 Å to interface atoms of each subunit. The accessible volume thus calculated at any element (x_i,y_i) allows for the inclusion of a solid with maximum cross-sectional diameter somewhat less than that of a water molecule. Hence, any element of the contact surface for which V_{ij} is ≤ 0 can be considered solvent inaccessible.

RESULTS

View of Phosphorylase a at 2.5-Å Resolution

The three-dimensional structure of the enzyme reveals it to be a highly specialized and well differentiated enzyme which nevertheless adheres to the same basic patterns of tertiary structure observed in simpler molecules. The subunit (Fig. 1) is organized into two domains. The N-terminal domain extends to a region near residue 490 and appears to be the general locus of allosteric regulation. The remainder of the chain forms the second domain which contains the covalently bound pyridoxal phosphate coenzyme and functions primarily in a catalytic role (41). The two domains exhibit similar α/β architectures (22) which consist of a central β-sheet core surrounded by α-helices. The catalytic cleft and the purine effector site are located between the domains. Glucose binds to the inactive (T) conformation of the enzyme at the active site as shown in Fig. 1.

Each momomer contains four sites at which positive effectors of the R state bind the enzyme and four at which negative effectors act. Three of these loci are held in common. The two interconverting enzymes, phosphorylase kinase and phosphorylase phosphatase, function as indirect "allosteric effectors", since phosphorylation of Ser-14 substantially reduces the difference in free energy between the T and R states (23, 24). Ser 14 is located near the N-terminus and lies at the subunit interface. The substrate G-1-P is itself a positive effector of the R state for both the *a* and *b* enzymes (12). This ligand binds at the active site, although to a different conformational state of phosphorylase (R) than does glucose (T). Under physiological conditions, the reaction favors glycogen degradation, and the enzyme is activated by glycogen at a predominantly α-helical storage site in the regulatory domain some 30 Å distant from the active site (25). No negative effectors are known to bind at this locus. P*b* is further dependent upon the presence of AMP at a positive effector site located at the intersection of two large helices in the regulatory domain within 10 Å of Ser-14 (26-28). ATP competes with AMP at this site and is a negative effector. P*a* and P*b* are subject to regulation by unknown negative effector(s) which bind to the enzyme at its surface ~10 Å away from the catalytic site (27, 29). In vitro, purine derivatives such as caffeine and inosine effect the R $\rightarrow$ T transition synergistically with glucose (29). The purine binding site is shared between the catalytic and regulatory domains and is nonexistent in the R form of the enzyme (27).

The phosphorylase dimer is remarkably asymmetric, possessing two distinct environments at the opposite ends of the twofold axis which relates the protomers (30). The "catalytic" face contains the glycogen storage site and is proximal to the active site cleft. This exposure of the dimer is presumably bound to the glycogen particle in vivo. The opposite, "control" face exposes the AMP binding site and Ser 14 and is thus available to activators and modifying enzymes. The interaction of these agents with the enzyme promotes profound conformational changes at the subunit interface which are functionally expressed as an allosteric transition.

The Dimer Interface

The total solvent accessible surface of a P*a* monomer buried by the subunit interaction has been calculated (31) and the results are summarized in Fig. 2. A remarkably small fraction

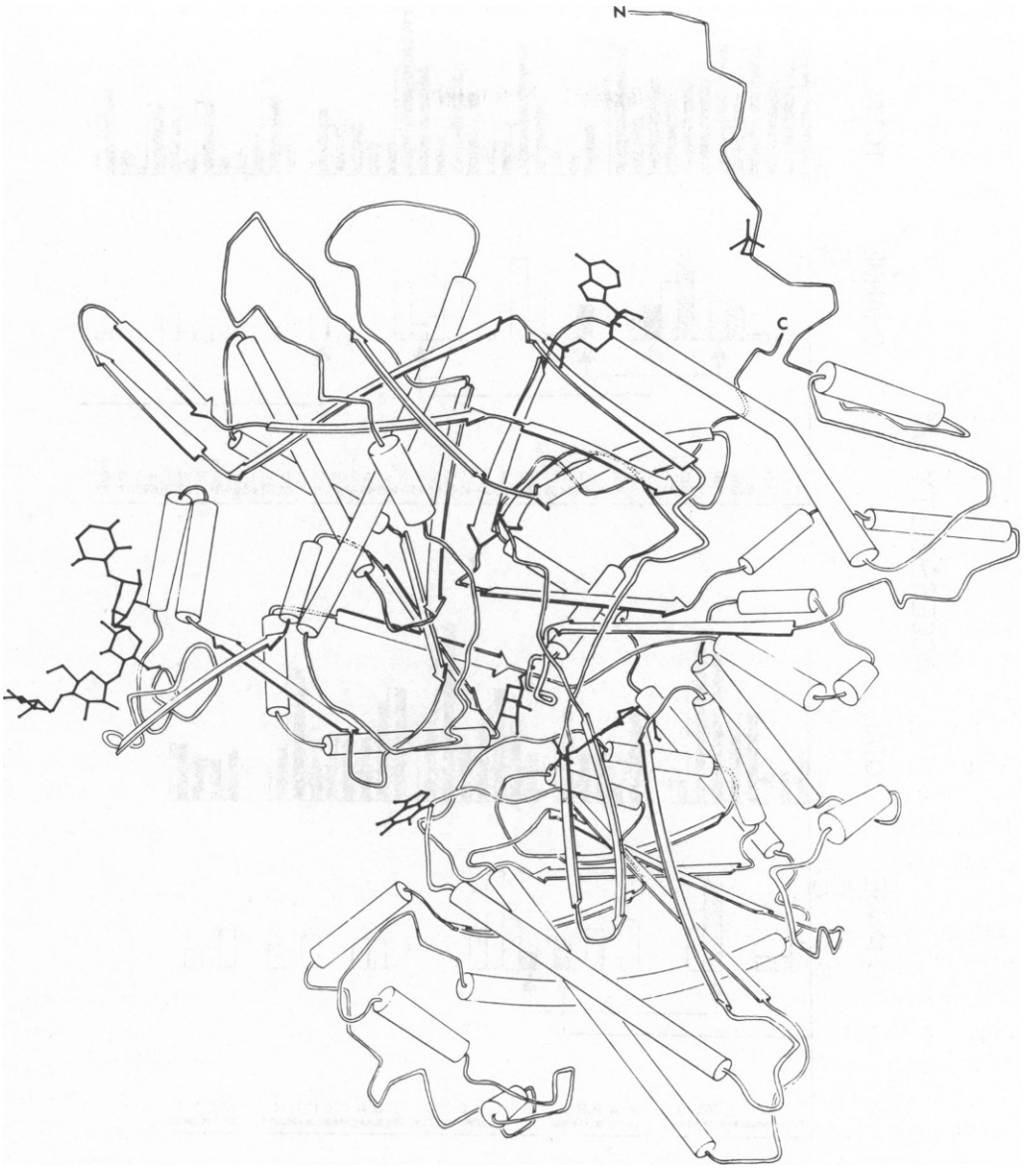

Figure 1 Schematic of phosphorylase *a* monomer. Cylinders and arrows represent α-helices and β-strands, respectively. Skeletal drawings are shown of ligands at their binding sites as determined by difference Fourier analysis: glucose (catalytic site), caffeine ("nucleoside", or negative effector site), AMP ("nucleotide", or positive effector site), and oligosaccharaide (glycogen storage and effector site). Ser-14-P and pyridoxal phosphate bound through the ϵ-amino group of Lys 679 are also shown.

of the molecular surface (6% of the total) is rendered inaccessible to solvent by subunit contacts. The value of $\Sigma\Delta A_s$ summed over all atoms of the dimer is 4,600 Å^2. The quantity ΔA_s is the difference in solvent accessibility between atoms of the dimer and two monomers with coordinates identical to those of one protomer of the dimeric molecule. Only 23 residues are rendered totally solvent inaccessible by placing the two monomeric models in contact. Summing over the atoms of these residues only, $\Sigma\Delta A_s$ is ~1,100 Å^2, about one quarter of the contact area. The graph of ΔA_s for interface residues with respect to sequence (Fig. 2) demonstrates that the contact region is highly localized even within the regulatory domain.

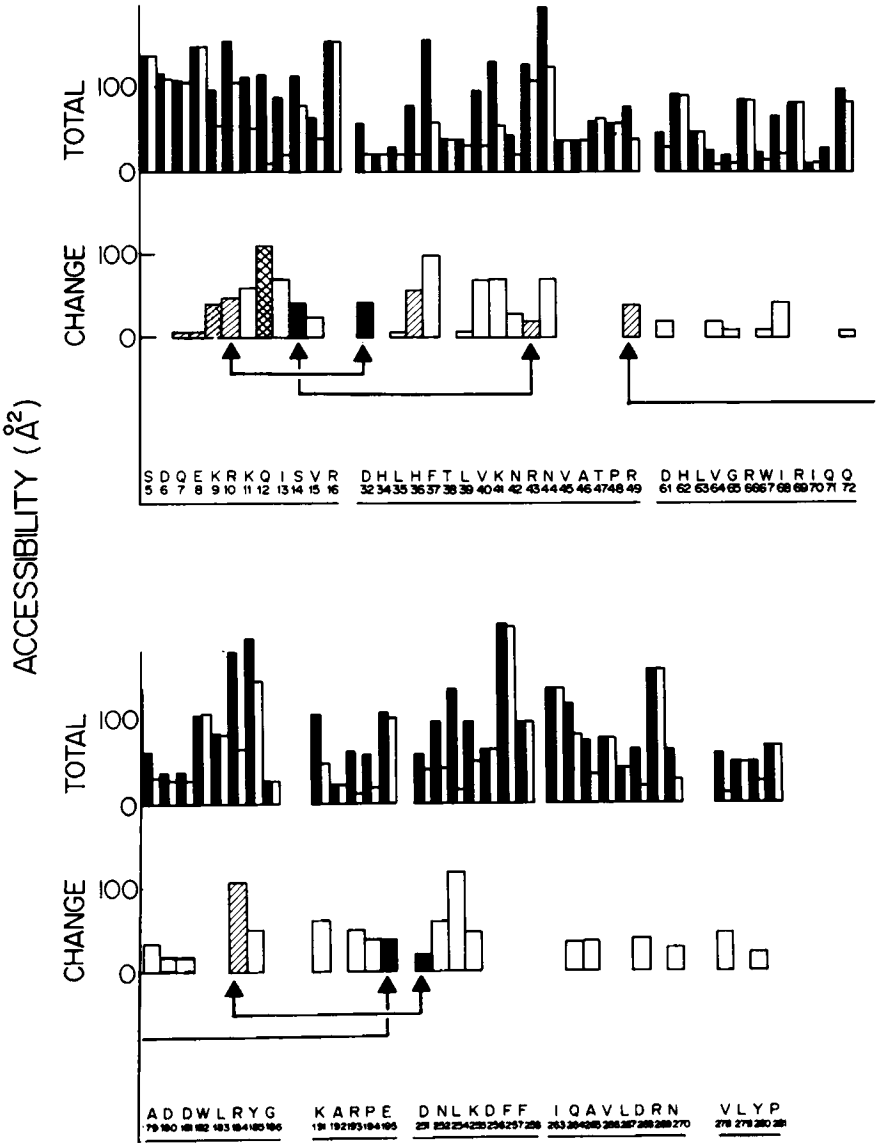

Figure 2 Solvent accessibility of residues at the dimer interface. Upper histograms show the total accessible surface area (Å^2) of interface residues: for an isolated subunit, i.e., using coordinates of only one protomer of P*a* dimer (black bars); for the same residues in the dimer (white bars). The lower histogram illustrates A_s (dimer)-A_s (monomer), the contribution of the subunit interaction to the withdrawal of interface residues from solvent. Bar pattern indicates the type of side-chain atoms buried: open bar, hydrophobic; black bar, negatively charged; diagonally-hatched bar, positively charged; cross-hatched bar, other polar. Arrows connect salt-bridged residues. Note that Arg 49 and Glu 195 are linked. Abscissa is labeled with residue number and its one-letter code.

More than half of the contacts involve the 50 N-terminal residues. It is striking that the involvement of main-chain atoms in subunit interactions, as estimated from ΔA_s, is insignificant. At the center of the subunit contact region, and completely surrounded by contacting residues, lies an island of solvent, ~2,000 Å^3 in volume (Fig. 3 *a*). This intersubunit space, which can accommodate 150–180 water molecules, would be inaccessible to external solvent in a static T structure.

Approximately 40% of the atoms for which solvent accessibility is restricted at the interface are polar, i.e., nitrogen or oxygen atoms. Contact maps (Figs. 3 *a–c*) of the subunit interface superimposed on the sum function show the position of atoms on one subunit surface which are within 4.0 Å of corresponding atoms on the opposing subunit. Contacts in which polar atoms participate are mapped in Fig. 3 *a* and nonpolar interactions involving carbon are shown in Fig. 3 *b*. Polar contacts tend to be clustered. Within these clusters, unambiguous identification of interacting pairs is usually not possible. It is immediately evident from the maps shown in Fig. 3 that polar interactions are distributed about the periphery of the subunit interface, whereas nonpolar contacts are also distributed throughout the interior of the contact region. About 100 total polar and nonpolar interactions are observed between the subunits. Only a quarter of these are contacts between polar atom pairs. This, with the accessibility data, would suggest that nearly 40% of the polar atoms at the interface are involved in dispersion forces with nonpolar (carbon) atoms.

There are four intersubunit salt bridges at the subunit interface (Fig. 3 *c*, 4). Two of these (Arg 10/Asp 32, Ser 14P/Arg 43) organize or anchor the N-terminal strand of one monomer to the first unit of α-helical secondary structure (Ile 20-Val 49) of the symmetry-related monomer. A third pair (Arg 49/Glu 195) is an α-helix/β-strand interaction which establishes a connection between the N-terminus and β-sheet core (Fig. 1) while the contact (Arg 184/Asp 251) is a β-strand/β-strand bridge between the β-sheet cores of the protomers. These salt bridges are distinguishable by their respective solvent accessibilities (Table I). With the exception of Asp 32, the two salt bridges which exclusively organize the N-termini are moderately accessible within the T-conformation dimer. The remaining two are significantly less so. The distribution of polar and nonpolar interactions can now be seen to cluster about the more accessible salt bridges, (Fig. 3) possibly providing them with enhanced stability at the surface of the dimer-solvent interface. The salient features of the dimer interaction can be summarized: (*a*) Only the regulatory domains are in contact. (*b*) The majority of polar and nonpolar interactions are clustered about two moderately exposed salt bridges which organize the N-termini. (*c*) The β-sheet cores of the two protomers are linked by less accessible salt bridges. (*d*) There is a cavity at the core of the interface with a solvent accessible volume of 2,000 Å^3.

Subunit Interactions in Phosphorylation b

The rms difference in scattering amplitude between crystals of P*a* and P*b* is 14% at 6-Å resolution (16). This implies that the two structures are not entirely homologous. Although a detailed comparison of the two enzymes has not been made at high resolution, a difference Fourier calculation incorporating 6.0-Å resolution data has been reported (16). Later analysis of these results revealed that a section of polypeptide from the N-terminus extending about 17 residues is disordered in P*b*[2], but no other significant features related to protein structural differences could be discerned. Johnson and collaborators have confirmed the disordered position of the N-terminus in subsequent studies (15).

Three ionic bonds help anchor the N-terminus to the P*a* dimer. In addition to the salt bridges involving Ser-14-P and Arg 10 in intersubunit contacts, Ser 14 is linked to Arg 69 at an α-helical unit within the monomer (Fig. 4). All of these potential interactions are lost by dephosphorylation of the enzyme and disordering of its N-terminus in the crystals. We think these results hold in solution as well.

---

[2]Fletterick, R. J. Unpublished observation.

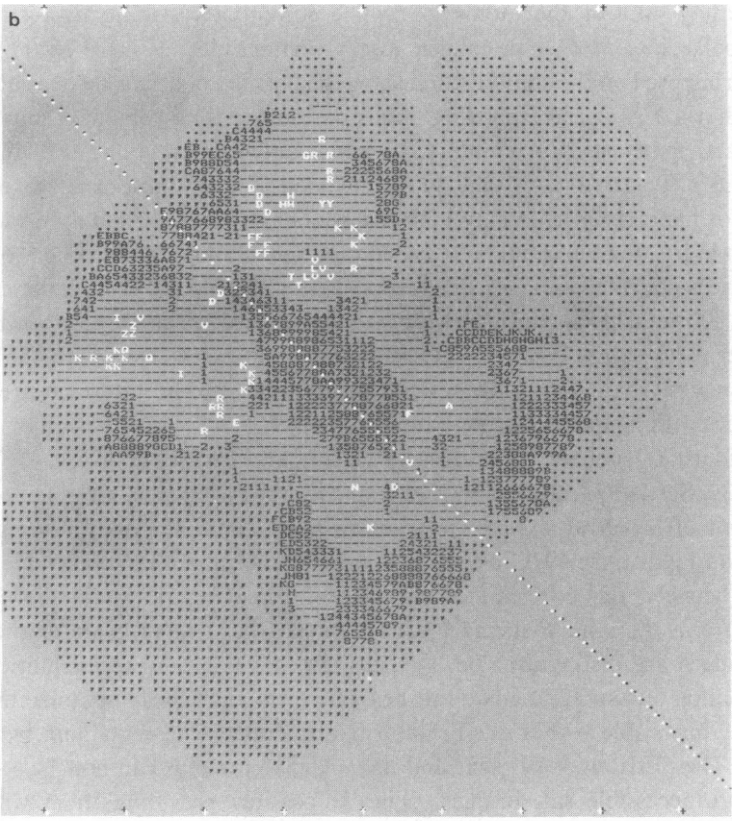
b

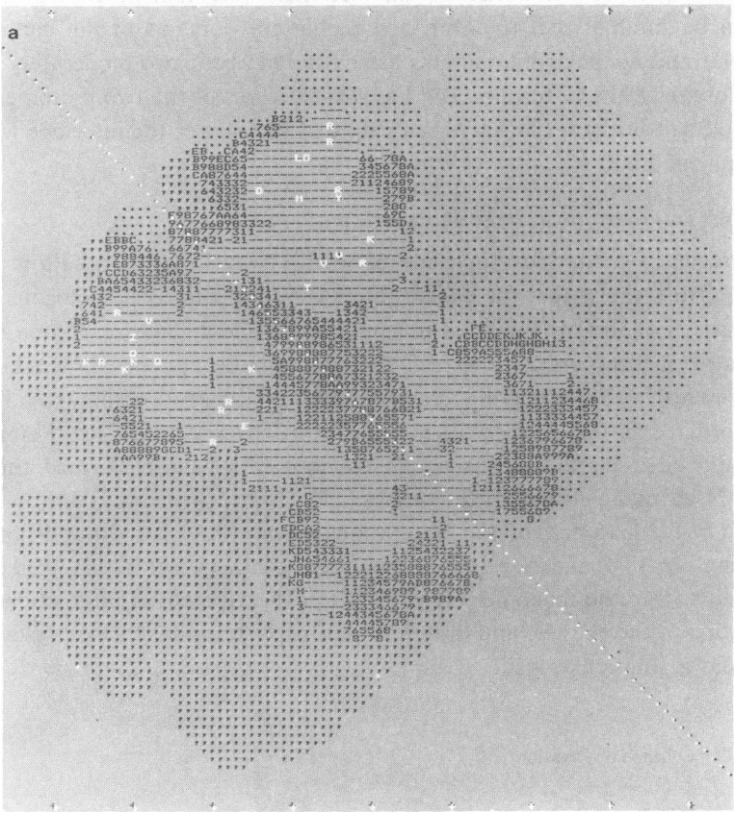
a

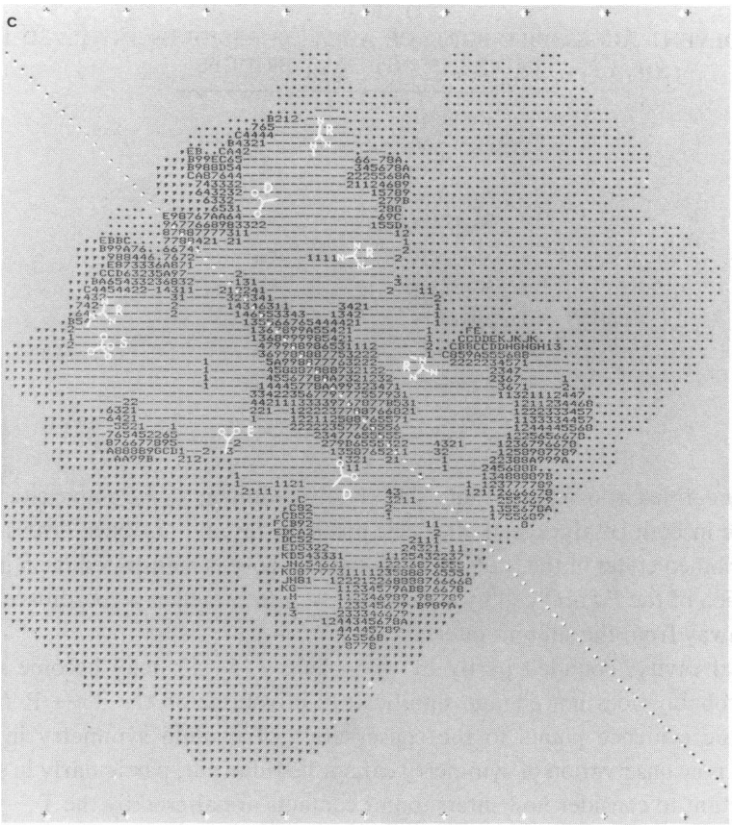

Figure 3 Sum function representation of the dimer interface. The solvent accessible volume is mapped in Å^3. The function is calculated in grids of 1 Å^2 so that map values can also be read as vertical displacement between subunits. The contribution of a solvent "probe" at the interface was included in the calculation (see Methods). Thus, map values represent the vertical distance between subunits exclusive of one water diameter. The value (−) indicates subunit contact; values (A,B,...) represent volumes (distances) (10, 11, ..., Å^3]). Monomer surfaces not "buried" or eclipsed are represented by (·) for one monomer and (,) for the other. The twofold axis relating the protomers is shown by the dotted line.

(*a*) Positions of polar atoms on one monomer which are involved in polar interactions are mapped by residue name (one-letter code) in white. (*b*) Positions of atoms involved in nonpolar contacts. (*c*) Charged groups of residues involved in salt linkages are drawn schematically.

Conformational Changes at the Subunit Interface: The T → R Transition

When crystals of P*a* are activated by allowing substrates to diffuse into the lattice, profound structural changes are observed in the molecule (17). The extent and magnitude of the conformational transition is shown quantitatively as a function of the magnitude of the gradient of difference electron density $|\nabla(\Delta\rho)|$ between R and T P*a* at 6.0-Å resolution (Fig. 5). The most significant changes are localized in the regulatory domain and particularly involve the lengthy α-helix spanning residues 45–75, and a complex unit of secondary structure (250–290) containing a short α-helix at the subunit interface and a loop (282–286) which is near the phosphate binding site. This loop and several residues (primarily Tyr 612) of the catalytic domain form the purine binding site in the T conformer. The data suggest that the N-terminal helix moves into the core of the enzyme with a rigid translation of ~ 5 Å. The Ser-14-P may move with the helix in this transition. Recall that in T state P*a* it is observed that in addition to intersubunit contacts, Ser-14-P forms a salt bridge with Arg 69 of this helix. Other structural changes are observed over the β-sheet core of the regulatory domain,

TABLE I
SOLVENT ACCESSIBLE SURFACE AREA OF RESIDUES INVOLVED IN INTERSUBUNIT SALT BRIDGES

Residue	A_s
	($Å^2$)
Arg10	107
Asp 32	19
Ser 14 P	78
Arg 43	110
Arg 49	75
Glu 195	62
Arg 184	72
Asp 251	42

but are poorly defined at 6-Å resolution. The chain movement at the active site region has an important role in both catalytic and allosteric mechanisms and has been discussed elsewhere (17). The combined effect of the transitions discussed above is manifested in an increase in the *c*-axis dimension of the P*a* unit cell by at least 2.0 Å, interpreted as a coordinate movement of the subunits away from the subunit interface.[3]

The central cavity, bounded partly by the α-helix (45–75), may become narrower and deeper but probably does not change significantly in volume on the T → R transition. All crystallographic evidence points to the conservation of twofold symmetry in the T → R transition but nonconservation of symmetry cannot be ruled out, particularly in solution.

It is important to consider how intersubunit contacts are altered by the T → R transition. The low resolution difference Fourier map is not of sufficient quality to allow displacement vectors to be determined for individual side chains. At best, it is only possible to determine whether both chain segments involved in a pairwise interaction undergo translation. In Fig. 5 regions of polypeptide chain which partake in subunit contacts are mapped on the function of $|\nabla(\Delta\rho)|$ vs. sequence number.

It is readily apparent that the subunit interface is profoundly affected by conformational change. The 70 residues of the N-terminus are presumed to move in a coordinate fashion; consequently, it is reasonable to assume that the salt bridge and associated interactions within the 70 residues are conserved by the T → R transition. In fact, there is some basis for believing that ordering of the N-terminus is an event in the activation pathway (see below). The fate of other intersubunit interactions is less clear. Arg 184 does not appear to be affected by the transition, as $|\nabla(\Delta\rho)|$ is well below the average value for the function, whereas Asp 251 lies in the midst of a "moving" α-helix. This does not imply that the salt bridge is broken; at the least it indicates side chain reorientation. Both Arg 59 and Glu 195 are involved in the structural change. Their interaction is not necessarily maintained.

DISCUSSION

The most distinctive feature of the P*a* subunit interface is the aggregation of salt linkages and other nonbonded contacts at the N-terminal residues of the regulating domains. A stable interaction of residues 1–20 with the α-helical array of the symmetry-related monomers

[3]Fletterick, R. J. Unpublished observation.

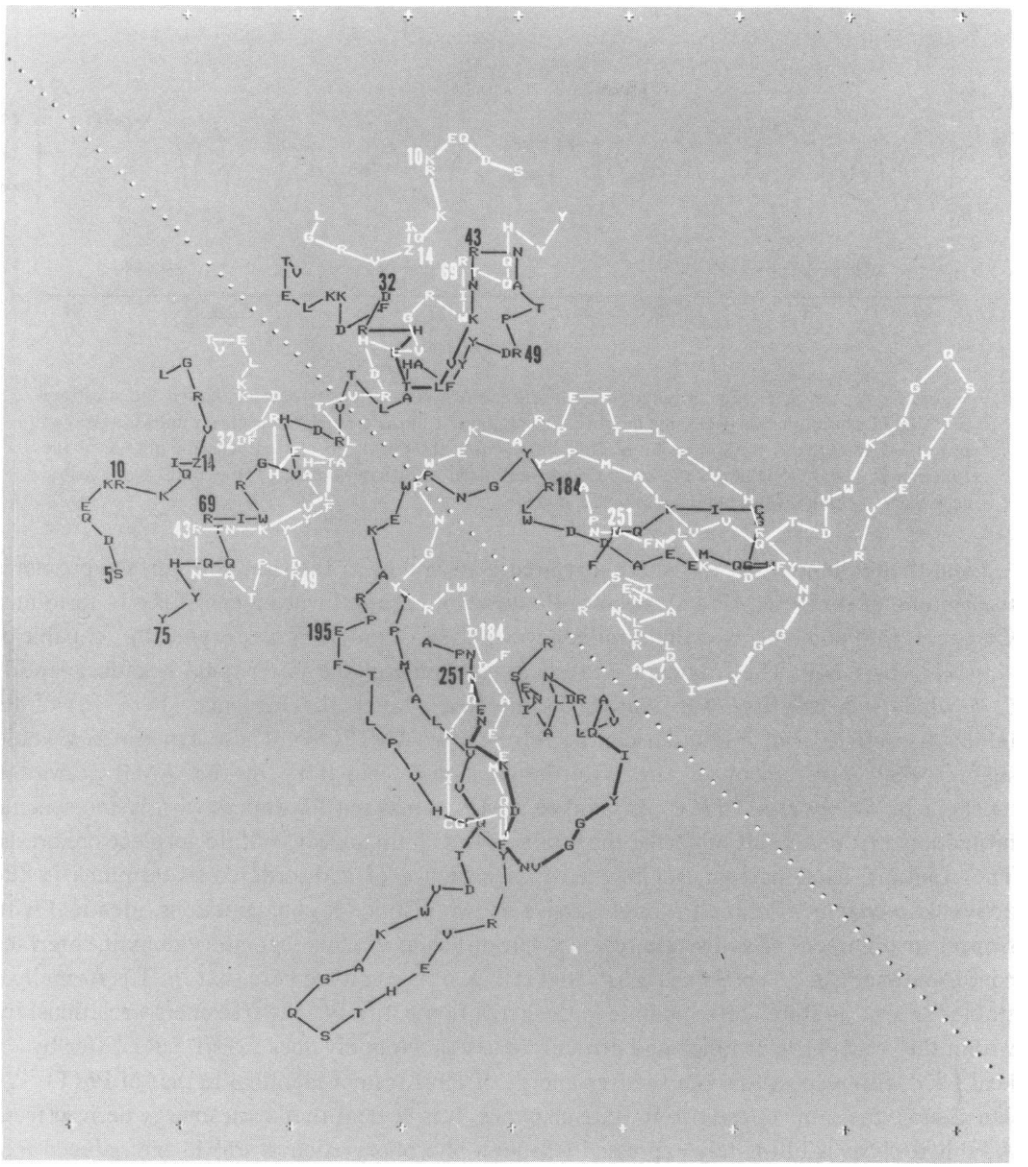

Figure 4 Connectivity of residues near the dimer interface. The α-carbon atoms of one monomer are shown in white; those of the symmetry mate are shown in black. Salt-bridged residues are indicated by number, as are Ser 5 at the N-terminus and Tyr 75 at the C-terminus of the helix (45–75).

requires (in the absence of effectors) phosphorylation of Ser 14. It has been demonstrated crystallographically that the N-terminus of P*a* is ordered (14), while that of P*b* is not (15). Both forms of the enzyme can be activated; however the equilibrium constant L for the intraconversion T $\rightarrow$ R is 3,000 for P*b* but only 3 for P*a* (23). Thus, tight intersubunit contacts involving the N-termini reduce the free energy barrier to activation by ~4 kcal. We can imagine the N-terminus to behave as an intramolecular allosteric effector of the R state organizing the subunit interface. This "effector" must be phosphorylated to bind at the dimer surface. Hence, P*b* is not activated by its N-terminus but depends, rather, on AMP for allosteric activation.

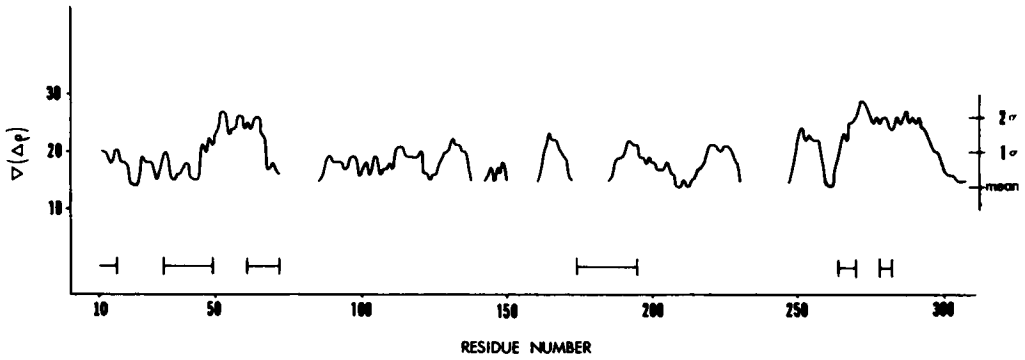

Figure 5 A moving average of the gradient of difference electron density between native and substrate perturbed P*a* as a function of residue number. The magnitude of the gradient in arbitrary units is averaged over 10 consecutive α-carbon positions. Only values over the mean are plotted. The magnitude of the function at 1 and 2 SD above the mean are shown in the right-hand ordinate. Horizontal bars enclose sequences of chain involved in intersubunit contacts.

Even though binding of the phosphorylated N-terminus at the subunit interface promotes the binding of AMP, AMP activation of P*b* does not require involvement of the N-terminus. Cori et al. (32) demonstrated that limited trypsinolysis of P*b* yields an enzyme, P*b*′, capable of activation by AMP. The fragment cleaved consists only of the N-terminal hexadecapeptide (33) which includes Ser-14-P. Antibodies directed against the sequence (1 → 18) of P*a* inhibit its activity, but inhibition can be reversed by AMP (34). These experiments would suggest that involvement of the N-terminus is not obligatory in the AMP activation mechanism. Gusev et al.[4] have cross-linked AMP complexed P*b* dimers with lysine specific bifunctional reagents and subjected the products to sodium dodecyl sulfate gel electrophoresis. The resulting band pattern is interpreted as evidence of a disordered N-terminus in the activated *b* enzyme. P*a* and P*b* might arrive at two distinct R conformations, identical with respect to alignment of active site residues but differing in their regulatory domain-interface conformations. Such a scheme is illustrated in Fig. 6. We can see here that P*a* T is formally a stable "transition state" intermediate in the activation pathway. The free energy relationships within this system are complex and difficult to assess. Not only does ΔG (T / R) differ by ~4 kcal for *a* with respect to *b* but the free energy of P*a*(T) is not identical to that of P*b*(T). We can assume the same of the two R-state enzymes. It is evident that some energy derived from ATP hydrolysis is ultimately expressed (through phosphorylation of P*b*) in the reduced free energy barrier to R in the *a* enzyme.

Although N-terminus and AMP may activate the enzyme independently, it is certain that AMP promotes the organization of the unphosphorylated N-terminus at the dimer interface to yield a homotropically cooperative P*b* dimer (12). Graves et al. (35) demonstrated that, unlike P*b*, P*b*′ is devoid of homotropic cooperativity with respect to AMP. We propose that the N-terminal residues are an essential vehicle through which conformational changes are transmitted across the dimer interface. Reference to Fig. 2 reveals that regions of secondary structure in the regulatory domain are sequentially linked across the subunit interface. The residues of the N-terminus are linked through three salt bridges and a majority of the remaining contacts are to the α-helix-loop-α-helix unit on the symmetry-related monomer. This α-helix (residues 45–72) is linked to the opposing α-sheet core via the salt bridge Arg

[4]Gusev, N. B., J. Hajdu, and P. Friedrich. Manuscript submitted for publication.

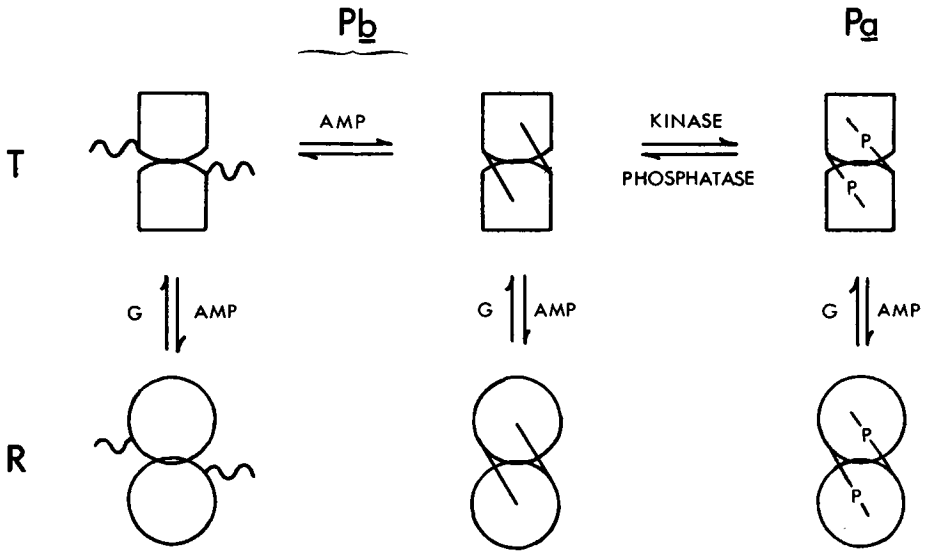

Figure 6 A tentative scheme for phosphorylase activation. P*b* (T) achieves the R state through AMP and substrate activation with (middle column) or without (left column) ordering the N-terminus. The latter mode does not effect homotropic cooperativity between subunits. Total ΔG (T→R) for P*b* is 4.8 kcal. Phosphorylase kinase (assumed to act on N-terminus ordered state of P*b*, but other pathways may be feasible) stabilizes, by phosphorylation of Ser-14, the interaction of the N-termini with the dimer surface, and reduces ΔG (T→R) by 4 kcal (right). P*a* (T) AMP 100-fold times more tightly than P*b* (T) (27) and activation proceeds by substrate and AMP as effectors. The R → T transition in all cases is effected by inhibitors such as glucose, G-6-P, or purines.

49–Glu 185. The core is in contact with a complex unit of secondary structure which forms subunit contacts through the packing of α-helices, and a contiguous loop (Asp 283 to Phe 285) which is involved in binding of both substrates and negative effector.[5] Upon activation, each of these connecting regions is affected by conformational changes which are ultimately expressed as catalytic competency in the enzyme. If the N-terminal 17 residues are to play a role in enzyme activation through the "transmission" of conformational perturbations, they must interact strongly at the interface region. Indeed, 1,000 square Å's of accessible surface area on the P*a* dimer are withdrawn from solvent by the binding of its N-terminus.

Phosphorylase kinase serves as a conformational trigger by introducing the charged phosphate group which strongly favors formation of salt bridges and subsequent ordering of the N-terminus. The driving force compensating for the entropy loss in the binding of the "intramolecular ligand" to the dimer surface is most probably the potential gain in solvent entropy, i.e., the hydrophobic effect (9). The salt bridges probably provide a favorable enthalpy of interaction as well. Noncomplementarity and possibly favorable solvent enthalpy prevent the stablilization of this interaction in P*b*. In that case, the free energy loss for both protein and solvent in solvating the charged and hydrophilic N-terminus (the sequence to Ser-14-P is Ac-S-R-P-L-S-D-Q-E-K-R-K-Q-I-S-14-P) apparently obviates the possibility of ordering the chain by a single salt bridge through Arg 10 and Asp 32. The three potential salt bridges form the basis for a cooperative folding unit in phosphorylase *a*. These additional salt bridges in P*a* are expressed as enhanced stability of dimers of that enzyme as opposed to dimers of P*b* (36).

[5]Watts, T., S. Sprang, and R. J. Fletterick. Unpublished results.

It remains to be answered how partly solvent accessible salt bridges can lower the free energy of binding. Perutz (8) has pointed out that charge pairs can be stabilized by fixed dipoles of the protein or of water molecules which minimize the free energy. Indeed, we observe a variety of potentially fixed dipoles in the form of polar interactions in the environment about the P*a* salt bridges. Estimations of the strength of individual salt bridges vary from 1 kcal/mol in hemoglobin (8) to 3 kcal/mol for an internal salt bridge in chymotrypsin (37).

The prevalence of salt linkages as a mode of intersubunit interaction may be characteristic of allosteric oligomers. The role of these forces is complex and not well understood. Despite a wealth of structural, kinetic and thermodynamic data concerning the T → R equilibrium in hemoglobin (5, 6), the molecular mechanism by which subunit interactions mediate the allosteric response is unclear. Subunit contacts in TMV disks involve two-salt bridge systems, one of which is extensive and implicated in the assembly process (7). Although the symmetry and packing of subunits in the icosahedral tomato bushy stunt virus and the tertiary structure of the protomers themselves differ radically from the TMV case (38), salt linkages appear to figure significantly in subunit interactions[6] and therefore, assembly.

A great variety of enzymes involved in many aspects of energy metabolism are regulated by phosphorylation in response to hormonal control (39). Phosphorylation can result in either activation (phosphorylase) or deactivation (pyruvate dehydrogenase). All of these systems are essentially allosteric, involving regulation by "another" site. The possible control of enzyme conformation by binding of an "intramolecular ligand," triggered by a phosphorylation step may be general and widespread in such systems.

A detailed understanding of this mode of allosteric regulation in phosphorylase must await a determination of a three-dimensional structure for the R conformer. Crystals of P*a* in this conformation have been prepared in our laboratory from shark muscle (40) and the structural studies are in progress.

This work was supported by the Medical Research Council in Canada and a grant #AM 26081 from the National Institutes of Health, U.S.A.

Received for publication 30 November 1979.

REFERENCES

1. Monod, J., J. Wyman, and J-P. Changeux. On the nature of allosteric transitions: a plausible model. *J. Mol. Biol.* **12**:88–118.
2. Adair, G. S. 1925. The hemoglobin system: the oxygen dissociation curve of hemoglobin. *J. Biol. Chem.* **63**:529–545.
3. Koshland, D. E., Jr. G. Nemethy, and D. Flimer. 1966. Comparison of experimental binding data and theoretical models in proteins containing subunits. *Biochemistry* **5**:365–385.
4. Koshland, D. E., Jr. 1959. Mechanism of Transfer Enzymes. *In* The Enzyme. Vol. 1. P. D. Boyer, and K. Myrback, editors. Academic Press, Inc., New York. 305.
5. Perutz, M. F. 1979. Regulation of oxygen affinity of hemoglobin: influence of structure of the globin on the hemoglobin. *Annu. Rev. Biochem.* **48**327–386.
6. Baldwin, J., and C. Chothia. 1979. Haemoglobin: the structural changes related to ligand binding and its allosteric mechanism. *J. Mol. Biol.* **129**:175–220.
7. Bloomer, A. C., J. N. Champness, G. Bricogne, R. Staden, and A. Klug. 1978. Protein disk of tobacco mosaic virus at 2.8 Å resolution showing the interactions within and between subunits. *Nature (Lond.).* **276**:362–368.
8. Perutz, M. F. 1978. Electrostatic effects in proteins. *Science (Wash., D.C.).* **201**:1187–1191.
9. Chothia, C. 1975. Structural invariants in protein folding. *Nature (Lond.).* **254**:304–308.
10. Hers, H. G. 1976. The control of glycogen metabolism in the liver. *Annu. Rev. Biochem.* **45**:167–189.

[6]Harrison, S. This volume.

11. Cohen, P. 1978. The role of cyclic-AMP-dependent protein kinase in the regulation of glycogen metabolism in mammalian skeletal muscle. *Curr. Top. Cell. Regul.* **14**:117–196.
12. Graves, D. J., and J. H. Wang. 1972. α-glucan phosphorylases—chemical and physical basis of catalysis and regulation. *In* The Enzymes. P. D. Boyer, editor. Vol. 7. Academic Press, Inc., New York. 435–482.
13. Fletterick, R. J., and N. B. Madsen. 1980. The structure and related functions of phosphorylase *a*. *Annu. Rev. Biochem.* In press.
14. Sprang, S. R., and R. J. Fletterick. 1979. The structure of glycogen phosphorylase *a* at 2.5 Å resolution. *J. Mol. Biol.* **131**:523–551.
15. Weber, I. T., L. N. Johnson, K. S. Wilson, D. G. R. Yeates, D. L. Wild, and J. A. Jenkins. 1978. Crystallographic studies on the activity of glycogen phosphorylase *b*. *Nature (Lond.)*. **274**:433–436.
16. Fletterick, R. J., J. Sygusch, N. Murray, N. B. Madsen, and L. N. Johnson. 1976. Low resolution structure of the glycogen phosphorylase *a* monomer and comparison with phosphorylase *b*. *J. Mol. Biol.* **103**:1–13.
17. Madsen, N. B., P. Kasvinsky, and R. J. Fletterick. 1978. Allosteric transitions of phosphorylase *a* and the regulation of glycogen metabolism. *J. BIol. Chem.* **253**:9097–9101.
18. Johnson, L. N., N. B. Madsen, J. Mosley, and K. S. Wilson. 1974. The crystal structure of phosphorylase *b* at 6 Å resolution. *J. Mol. Biol.* **90**:703–717.
19. Jack, A., and M. Levitt. 1979. Refinement of large structures by simultaneous minimization of energy and R factor. *Acta Crystallogr. Sect. A.* **34**:931–935.
20. Lee, B., and F. M. Richards. 1971. The interpretation of protein structures: estimation of static accessibility. *J. Mol. Biol.* **55**:379–400.
21. Greer, J., and G. Bush. 1978. Macromolecular shape and surface maps by solvent exclusion. *Proc. Natl. Acad. Sci. U.S.A.* **75**:303–307.
22. Levitt, M., and C. Chothia. 1976. Structural patterns in globular protein. *Nature (Lond.)*. **261**:552–558.
23. Helmreich, E., M. C. Michaelides, and C. F. Cori. 1967. Effects of substrates and a substrate analog on the binding of 5'-adenylic acid to muscle phosphorylase *a*. *Biochemistry* **6**:3695–3710.
24. Griffiths, J. R., N. C. Price, and G. K. Radda. 1974. NMR studies of glycogen phosphorylase. *Biochim. Biophys. Acta.* **358**:275–280.
25. Kasvinsky, P. J., N. B. Madsen, R. J. Fletterick, and J. Sygusch. 1978. X-ray crystallographic and kinetic studies of oligosaccharide binding to phosphorylase. *J. Biol. Chem.* **253**:1290–1296.
26. Fletterick, R. J., J. Sygusch, H. Semple, and N. B. Madsen. 1976. Structure of glycogen phosphorylase *a* at 3.0 Å resolution and its ligand binding sites at 6 Å. *J. Biol. Chem.* **251**:6142–6146.
27. Kasvinsky, P. J. N. B. Madsen, J. Sygusch, and R. J. Fletterick. 1978. Phosphorylase *a* by nucleotide derivatives. *J. Biol. Chem.* **253**:3343–3351.
28. Johnson, L. N., E. A. Stura, K. S. Wilson, M. S. P. Sansom, and I. T. Weber. 1980. Nucleotide binding to glycogen phosphorylase *b* in the crystal. In press.
29. Kasvinsky, P. J., S. Shechosky, and R. J. Fletterick. 1978. Synergistic regulation of phosphorylase *a* by glucose and caffeine. *J. Biol. Chem.* **253**:9102–9106.
30. Fletterick, R. J., S. Sprang, and N. B. Madsen. 1979. Analysis of the surface topography of glycogen phosphorylase *a*: implications for metabolic interconversion and regulatory mechanism. *Can. J. Biochem.* **57**:789–797.
31. Sprang, S., D. Yang, and R. J. Fletterick. 1979. Solvent accessibility properties of complex proteins. *Nature (Lond.)*. **280**:333–335.
32. Cori, C. F., and G. T. Cori. 1943. Crystalline muscle phosphorylase: kinetics. *J. Biol. Chem.* **151**:39–47.
33. Fischer, E. H., D. J. Graves, E. R. S. Crittenden, and E. G. Krebs. 1959. Structure of the site phosphorylated in the phosphorylase *b* to a reaction. *J. Biol. Chem.* **234**:1698–1704.
34. Janski, A. M., and D. J. Graves. 1977. An antibody probe for the amino-terminal region of glycogen phosphorylase. *FEBS (Fed. Eur. Biochem. Soc.)*. **82**:232–236.
35. Graves, D. J., S. A. S. Mann, G. Phillip, and R. J. Olivera. 1968. A probe into the catalytic activity and subunit assembly of glycogen phosphorylase. *J. Biol. Chem.* **243**:6090–6099.
36. Graves, D. J., R. W. Sealock, and J. H. Wang. 1965. Cold inactivation of glycogen phosphorylase. *Biochemistry* **4**:290–311.
37. Fersht, A. R. 1971. Conformational equilibria and the salt bridge in chymotrypsin. *Cold Spring Harbor Symp. Quant. Biol.* **36**:71–73.
38. Harrison, S. C., A. J. Olson, C. E. Schutt, F. K. Winkler, and G. Bricogne. 1978. Tomato bushy stunt virus at 2.9 Å resolution. *Nature (Lond.)*. **276**:368–373.
39. Krebs, E. G., and J. A. Beavo. 1979. Phosphorylation-dephosphorylation of enzymes. *Annu. Rev. Biochem.* **48**:923–960.
40. Munn, M., S. Sprang, and R. J. Fletterick. 1979. Crystallographic studies of the activation of glycogen phosphorylase *a*. Abstr. Am. Crystallogr. Assoc. Meet., Hawaii. 63.
41. Sygusch, J., N. B. Madsen, P. J. Kasvinsky, and R. J. Fletterick. 1977. Location of pyridoxal phosphate in glycogen phosphorylase *a*. *Proc. Natl. Acad. Sci. U.S.A.* **74**:4757–4761.

DISCUSSION

Session Chairman: David Eisenberg *Scribe*: Laura Pologe

LEE: I'm a little confused about your position on the role of the N-terminus and AMP as effectors in the *b* enzyme. What is your assessment of the conformation of *b* enzyme? Is it in equilibrium where the N-terminus is tucked in and out, or is it in just one conformation?

SPRANG: The answer, I think, is that we don't know. A lot of people have been trying to come up with experimental methods to determine the state of the N-terminus of phosphorylase *b* upon activation, but I don't really know personally of any experiments which are at all definite. One could easily come up with at least two obvious models. One is that AMP, as an effector, is able to organize the N-terminus. The introduction of the phosphate group of AMP and possible stacking interactions with Tyr 75, for example, which is located at the C-terminus of the helix and figures largely in the conformational change, might stabilize an ordered structure for the N-terminus. We know that phosphorylase *b* shows homotropic cooperativity with respect to AMP binding. We know that if this molecule is trypsinized and the 17 N-terminal residues are removed, AMP can still activate the enzyme catalytically but that it loses its cooperativity. That might lead one to suspect that AMP somehow functions in the same role as serine phosphate. From the geometry of the enzyme it is not obvious how that could happen. Arg 43, one of the residues salt-bridged to serine-14 phosphate, is possibly involved in an interaction with the AMP phosphate.

FLETTERICK: It is difficult to answer that question but a number of people have tried. One thing we know is that this structure (phosphorylase *b*) which is inactive with or without the phosphate group, is more sensitive to proteolysis, and one of the major cuts is at amino acid 17. We presume in this case that by binding glucose, and this is the natural structure, that the flexibility in structures of the N-terminus is far greater than it is when undergoing this conformation change.

ALLEWELL: How did you estimate the energy change associated with the T-R transition?

FLETTERICK: It's estimated from the free energy change of the R-T equilibrium constant for phosphorylase *b* vs. phosphorylase *a*. It's ~4.5 kcal/mol without the phosphoserine and ~0.8 with the phosphoserine.

ALLEWELL: Is it derived from a Hill plot?

FLETTERICK: Yes. It's been derived by Ernst Helmreich from Hill plots and also from some of our own kinetics in Neil Madsen's lab.

ALLEWELL: Doesn't that make a lot of assumptions about the mechanism of the activation? What is the underlying evidence that it actually is a transition between only two states?

FLETTERICK: That is an excellent point. How many conformational states are really here? We have evidence in our lab for a large number. Fig. 6 is meant to simplify the process. For example, phosphorylase *a* with the phosphate group is not a fully active enzyme. You get an additional twenty percent activity by adding AMP. This is an example of a further stabilization of the active structure by the second ligand. In fact all of these kinetic measurements have a great deal of error in determining these equilibrium constants, so the error in ΔG is a kilocalorie or two. Numbers come out for ΔG for P*b* between 1,000 and 3,000, and for P*a*, between 3 and 20. There's still two orders of magnitude difference between them.

ACKERS: To what extent can you assign localized effects to parts of the molecule, when looking at the structural modification of a regulatory protein? You are talking here about effects which are possibly assignable to particular salt bridges. In the history of this issue, which has been studied extensively in hemoglobin as well as in many other systems in a more fragmentary way, there is a tendency first to look at structures and to attempt to assign conspicuous pairwise interactions and then to carry out chemical modifications or look at mutants which involve those particular interactions. When one does that one finds significant changes in the energetics of the system. To identify and then find such energies is sort of a procrustean approach. In thinking about these salt bridges, one might look in more detail at the thermodynamic parameters. In particular one could look at the enthalpies and entropies to see whether or not these are consistent with salt bridge formation. The free energies alone don't provide you with very much information in that regard.

FLETTERICK: Julian Sturtevant is looking at ΔCp's for this system at the moment. But it will probably take awhile because they're difficult experiments.

On another point, in addition to forming these R species as described (approximately) in Fig. 6, you can do it at the active site, or you can do it at yet a fourth site, i.e., you can start forming these species by binding oligosaccharide. Thus, you can do this activation at four different loci on the molecule and in fact, those sites can be integrated before you arrive at a "final" conformation. Biologically that is exactly what this molecule is meant to do. It's a transducer required to sample cellular metabolite levels and in fact provides a response to the cell. It's doing an integration over space over the surface of the enzyme, so I am the last one who would say that there are very specific points. What we want to do with this model is molecular dynamics.

LUMRY: With respect to Dr. Ackers' remark about thermodynamic models for ammonium group—carboxylate group ion pairs, there aren't any. I have checked with everybody who is in the business. These models always involve at least three bodies. They always involve at least one molecule of solvent. I'd give my left arm to have some good model data, but we don't. So when one starts talking about these salt bridges in terms of what they're worth in thermodynamic terms, it's the blind leading the blind.

SPRANG: I want to point out that as in some of these other systems that we've been looking at today, the important residues appear to be arginines that are complexing with the phosphate groups.

ROSS: Salt bridges are obviously electrostatic interactions and therefore depend on the dielectric constant of the medium quite strongly. So the question is, in your structure, what is the environment of these bridges?

SPRANG: The environment around the serine is to some extent solvent accessible and I know that you would expect from electrostatic consideration that the salt bridge should have a very small contribution to the total enthalpy. The whole business of thinking about bulk properties as they affect specific interactions involves terribly complicated questions.

FINNEY: There are a couple of fairly straightforward factual questions I'd like to ask. First, I'm very pleased to see you've noticed 40% of your polar atoms at the interface involved in apolar interactions, this figure agreeing with what we've found on the inside of proteins. Do you have any information as to whether those polar groups involved in polar-apolar contacts are already participating in hydrogen bonds or are accessible to solvent in any other way? Or are they groups in which the polar interactions to other polar interactions are being suppressed? Are they solvent accessible or are they also hydrogen bonded elsewhere?

SPRANG: Many of them are in fact completely buried.

FINNEY: And we don't know anything about their hydrogen bonding interaction?

SPRANG: We haven't attempted to assign hydrogen bonded pairs. We've only been looking at close contacts and accessibility changes. We have been talking about that region of the interface which is surrounded by solvent and has within it a pool of solvent that appears to be withdrawn from solvent at the interface.

FINNEY: I have another question. This large solvent filled hole you have: have you looked at the nature of the internal surface of this hole in terms of its polar-apolar nature?

SPRANG: Not carefully. If one looks at a Feldman type representation, there's an awful lot of red and blue in there. I haven't characterized it.

GERGELY: I wonder if you could clarify this idea that you have a subunit-subunit interaction across the interface and this has something to do with clustering. You have the two subunits always together as shown in your diagram, and the phosphorylation occurs in both. In what sense do you say that you are in fact going from one subunit to the other?

FLETTERICK: Biologically, what happens in this activation process is that as soon as the hormonal signal phosphorylates this enzyme, the ΔG is so small that it's virtually an active species, not an allosteric enzyme. An exception to that is when negative allosteric effectors are present. There are at least three here. Let's say that this is occurring in a background of glucose, which it does in liver, though not in muscle cells. Then this R/T equilibrium is pushed back into the T conformation and the allostery that we would talk about would be the two active sites. The active site on subunit one, when it's loaded with inorganic phosphate and saccharide, promotes binding of substrates at the second binding site, giving another picture: the structural change which you saw at the interface extends in fact to those active sites. This is very analogous, incidentally, to hemoglobin. But it is a fact that when we can stabilize the T structure, such as phosphorylase *a* with glucose, there is positive allosteric cooperativity between the substrate binding sites, and incidentally, also between the AMP sites. If it's phosphorylase *b*, you don't see cooperativity between AMP binding at the two binding sites per dimer; you see it only in a background of glucose.

B. K. LEE: Is ΔG of 4.5 kcal from after AMP is bound or without AMP?

SPRANG: Without.

ALLEWELL: I wonder why you said that phosphorylase *a* was no longer allosteric as a result of the free energy change being zero. According to the two state model, doesn't the property of allostery depend on differences in binding energies between the two states, and not the actual free energy of the transition?

FLETTERICK: The free energy of binding is such that we're confused about what the data are representing. In this T conformation we can't bind substrates in the P*a* crystal which would presumably promote this R structure. Louise Johnson, who works on this molecule, P*b*, in Oxford, can bind substrate and she does get enzyme in this T conformation. I'm quite confused about the energetics of this interaction. What we do know is that the Hill coefficient for AMP binding to phosphorylase *a* is 1. If you measure it in a background of glucose, it's 1.6. And it's 1.6 for this case, P*b*.

JENTOFT: I'm curious about the central cavity that you see. One, do you have any speculation on the role of that solvent cavity and two, are there polar groups that line that cavity?

SPRANG: On question two, there is reason to believe that the dimensions of that channel change within the R-T structural change. Question one: it's also possible to imagine that it's a good way to diffuse phosphate ions into or towards the active site.